

Research Article



Computed Tomography Findings of Inflammatory Myofibroblastic Tumors Arising in the Abdominopelvic Region

Huijuan Xiao^{1#}, Hongna Tan^{1#}, Fengchang Bao², Yonggao Zhang¹, Bo Wang¹, Jianbo Gao^{1*}, Wei Liu²

Department of Radiology, The First Affiliated Hospital of Zhengzhou University, Zhengzhou University, Henan, China, 450052

Department of Hematology, Children's Hospital of Zhengzhou City, Zhengzhou, 255 Gangdu Road, Henan, China, 450000

Authors Huijuan Xiao and Hongna Tan contributed equally to this report.

*Corresponding author: *cjr.gaojianbo@vip.163.com*

Abstract

Purpose: To describe the clinical, CT findings of abdominopelvic inflammatory myofibroblastic tumor (IMT) to enhance the recognition of this rare disease. **Materials and Methods:** The clinical, CT findings of 14 patients with IMT conformed by pathology in the abdominal and pelvic regions were retrospectively reviewed. **Results:** Ten of 14 patients had solitary lesions. On plain CT images, a soft tissue mass was found in all IMT lesions, except for one lesion arising in the small intestine. After contrast administration, all soft tissue masses were persistently enhanced heterogeneously with various cystic regions, including 9 cases with markedly enhancement and each two cases with moderate, slight enhancement. Of the 9 cases with markedly enhanced lesions, large-area cystic changes were found in 3 cases, which were located at the kidney, bladder, pelvic cavity and inguinal region; multiple ring-shaped enhancements in one case developed in the mesentery, and one lesion occurred in the inguinal region and showed a markedly enhanced mass, mimicking castleman's disease. Two slightly enhanced lesions originated in the retroperitoneal region. Five of the 14 IMT patients showed invasion into adjacent structures. **Conclusion:** The CT characteristics of IMT are various owing to different locations, and the final diagnosis depends on the histopathology.

Keywords: Inflammatory Myofibroblastic Tumor; Abdominopelvic Region; Computed Tomography; Pathology

Introduction

Inflammatory myofibroblastic tumor (IMT) is a rare tumor of mesenchymal origin. In the past, this entity was described as a plasma cell granuloma, fibrohistiocytoma, inflammatory pseudotumor, fibroxanthoma, or inflammatory fibrosarcoma, among other names (1-3). According to the 2002 WHO classification of soft tissue tumors, IMT was finally defined as a disease that mainly consists of myofibroblastic spindle cells with variable infiltration of plasma cells and/or lymphocytes (4). The exact etiology of this rare disease is still unknown.

Clinically, the symptoms and manifestations of IMT depend on the location of the lesions. IMT can occur

at anywhere in the body, and the lung is the most common site of involvement. Although most IMT cases have a good prognosis after surgical resection, some cases have malignant potential and may be locally aggressive and recrudescence; distant metastasis may also occur in rare cases (2, 3, 5-10). The abdomen and pelvic regions are the most common locations of extrapulmonary IMT (2, 3, 8), but some cases show large and irregular intra-abdominopelvic masses with more aggressive growth patterns, mimicking sarcomas.

The clinical and pathological characteristics of IMT are well known, but the radiological characteristics of

IMT with locations in the abdominopelvic region have been reported in only a few studies, most of which are case reports (5-7, 9-15). Therefore, this report describes the clinical features, computed tomography (CT) and pathological findings of 14 patients diagnosed with IMT in the abdominopelvic region to enhance the recognition of this disease and help differentiate it from other types of abdominopelvic tumors.

Materials and Methods

Patient population

The clinical and imaging records of 14 patients with the approval of the local ethics committee and informed consent provided, which were confirmed as IMT between Sept. 2009 and Oct. 2013, were retrospectively reviewed. All patients had preoperative CT records, including one plain CT scan and 13 plain and contrast-enhanced scans. There were 8 female and 6 male patients with an age range of 16 months to 84 years (mean: 45.8 years old). Of these 14 IMT patients, 8 cases presented with a mass in the abdominal and pelvic regions, 4 patients with lesions located at the sites of gastrointestinal tract showed abdominal pain and distension, and two patients with lesions arising in the bladder and vesicorectal space presented with intermittent gross hematuria. There was one case of postoperative recurrence in our study. The duration of the symptoms was between several days and 2 years. Twelve cases were confirmed by surgery and two by core needle biopsy pathology. All of the pathologic specimens were reviewed by pathologists for routine H&E staining and immunohistological staining for immunological markers. The immunological markers that were assessed included vimentin, desmin, smooth muscle actin (SMA), muscle specific actin (MSA), anaplastic lymphoma kinase (ALK), myogenin and CD34.

Imaging techniques

All 14 patients with confirmed IMT underwent computed tomographic scans using a Somatom Sensation Cardiac 128-slice CT (Siemens Medical Systems, Erlangen, Germany) helical scanner. The scan parameters were as follows: 5 mm slice thickness reconstructions, 45 cm field of view, 120 kV voltage, 200 mA, and 512×512 matrix. Three-dimensional

(3D) CT images were reconstructed using the InSpace software (Siemens LEONARDO Workstation). One patient underwent plain CT scanning, and the remaining thirteen patients underwent plain and contrast-enhanced CT scanning. An intravenous bolus dose of 100 ml of a nonionic iodinated contrast agent, iopromide (Ultravist, Bayer Schering Pharma AG, Berlin, Germany), was administered to the patients who underwent enhanced CT scanning at a rate of 3 mL/s, which was followed by a 20 ml saline flush. Arterial phase and venous phase images were obtained; imaging was performed 60 s and 105 s after contrast material injection.

Imaging interpretation

Two experienced radiologists with five or more years of radiological experience independently reviewed all of the patient CT images. The radiologists were blinded to the final pathological results, and the final assessment was reached by consensus through discussion. The aspects of the tumor that were described on CT included the tumor location, size, morphology, and margin (well-defined or ill-defined) as well as the CT density (hypo-, iso-, or hyper- dense in relation to the adjacent muscle density), calcification, contrast enhancement appearances (homogeneous or heterogeneous), lesion texture (homogeneous, or heterogeneous, or necrosis), and the conditions of the adjacent tissue structure and distant metastasis at diagnosis. We then compared the imaging findings with the pathological results.

Results

The clinical and pathological findings of these 14 IMT patients with lesions arising in the abdominal and pelvic region are shown in Table 1. Of these 14 IMT patients, the lesions of 10 cases were solitary, including those in the gastrointestinal tract (n=3, each, including one case of ileum, ileocecum and small intestine), retroperitoneum (n=2), and one case each in the vesicorectal space, mesentery, kidney, inguinal region and bladder. The remaining 4 patients had multiple lesions, including two cases with sites in the pelvic cavity and abdominal wall, and one case each in the pelvic cavity and inguinal region, presacral region and buttocks. The size could not be measured in 4 cases of multiple lesions and one case located at the small intestine because of the appearance of bowel

wall thickening; of the remaining 9 single lesions, the maximum diameter ranged from 3.2 cm to 18.8 cm, with a mean maximum diameter of 7.2 cm. Histologically, all of the tumors predominately consisted of myofibroblastic spindle cells accompanied by a variable inflammatory cells; and the immunohistochemical examination revealed 100% (14/14) of the lesions had consistent positive staining for SMA, and there was positive staining with CD34 in 7 cases (50%, 7/14), with vimentin and ALK in 5 cases each (35.7%, 5/14), with MSA and desmin in 4 cases each (28.6%, 4/14), and myogenin in two cases (14.3%, 2/14).

All 14 patients underwent CT scanning, including one plain CT scan and 13 plain and contrast-enhanced scans. The CT findings are listed in Table 2. On plain CT images, a soft tissue mass was found in all IMT lesions, except for one lesion that arose in the small intestine, appearing as focal thickening in the bowel wall (Fig. 1). Of these 13 cases of mass-like lesions, 4 patients with multiple lesions were included (Fig. 2a); 69.2% (9/13) of the lesions had an irregular shape (Fig. 3), an oval shape was found in 3 patients (Fig. 4a), and a fusiform shape occurred in one patient (Fig. 5); 61.5% (8/13) of the lesions had an ill-defined margin. Of these lesions in 14 patients with IMT, 71.4% (10/14) of the lesions showed isodensity, and the other 4 cases had low density; 8 cases demonstrated heterogeneous density, including 7 cases with cystic changes and one patient with hemorrhagic changes (Fig. 4a). No calcification was found in our study. After the administration of a contrast agent, all soft tissue masses were persistently enhanced; they were heterogeneous with various cystic regions, including 9 cases that were markedly enhanced and each two cases with moderate, slight enhancement. Of the 9 cases with lesions that were markedly enhanced with various cystic regions, large-area cystic changes were found in 3 cases that located at the kidney, bladder, pelvic cavity and inguinal region (Fig. 4b; Fig. 6); multiple ring-shaped enhancements in one case arose in the mesentery (Fig. 7), and one lesion in the inguinal region had a markedly enhanced mass, which was misdiagnosed as castelman's disease (Fig. 8). The remaining 4 lesions showed heterogeneous enhancement with a small, cystic area. Two slightly enhanced lesions originated in the retroperitoneal region (Fig 9). Of two moderately enhanced cases, one case was a recurrent lesion of the left buttocks (Fig 2b), and the other was a lesion in the ileum (Fig 5).

Of these 14 IMT patients, 5 cases showed invasion into adjacent structures, including all four patients with multiple lesions and a single lesion located at the vesicorectal space (Fig. 2b, Fig. 10), and the positions of invasion included the bladder wall, adjacent intestinal canal, muscle or skin. The complications of intussusception and pelvic effusion were found in a patient with a lesion located at the ileum (Fig. 5), and bilateral kidney and ureter expansion were found in a patient with a lesion arising in the vesicorectal space (Fig. 10). For that lesion, peripheral structures were shifted by a huge renal mass (Fig. 4).

Discussion

Inflammatory myofibroblastic tumor (IMT) was first described as a plasma cell granuloma in the lung by Bahadori and Liebow in 1973 (1), and it has now been identified at multiple extrapulmonary locations (2). Because of the confusion about the histogenesis of this disease, there have been many synonyms for IMT, including inflammatory pseudotumor, plasma cell granuloma, fibrous histiocytoma and fibroxanthoma (1-3); inflammatory pseudotumor was the most frequently used name. The use of 'inflammatory myofibroblastic tumor' was introduced after myofibroblasts were eventually recognized as the principal spindle-cell types in the inflammatory pseudotumor (16, 17). The exact etiology of this rare disease is still unknown. Whether IMT represents a reactive or neoplastic process was previously controversial, but it was recently proven to be a true neoplasm through oncocyto-genetics (18, 19). Additionally, the tumor has been confirmed to have anaplastic lymphoma kinase (ALK) gene rearrangements located on chromosome 2p23, resulting in the over-expression of ALK protein (20). In addition to the ALK gene abnormalities, IMT is may have a relationship with infection, vascular issues, or autoimmune disorders. Because some IMT cases have malignant potential and may be locally aggressive, recrudescence, and rare distant metastasis (2, 3, 5-10), IMT is currently considered a low grade malignant or intermediate tumor consisting of spindle cells with variable infiltration of inflammatory cells on histopathology (4).

IMT can occur virtually anywhere, and the lung is the most commonly involved site; extrapulmonary locations have also been reported in the abdominal and pelvic cavity, head and neck, and meninges (5-7, 9-15,

Table 1 Clinical and Pathological Findings in 14 Patients with IMT

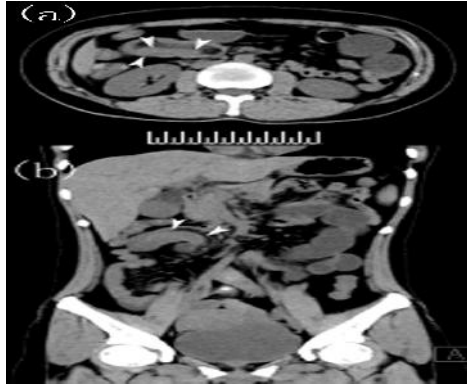
Case	Age	Sex	Location	Size/cm	Vimentin	Desmin	SMA	MSA	ALK	Myogenin	CD34
1	39 years	male	ileum	5.5	+	-	+	-	-	-	-
2	9 years	female	pelvic cavity and abdominal wall	Not be measured	-	-	+	-	-	+	+
3	56 years	male	retroperitoneal	5.0	-	-	+	-	-	-	-
4	84 years	male	ileocecus	6.4	-	+	+	+	+	-	-
5	16 months	female	kidney	12.6	+	-	+	+	-	+	+
6	39 years	female	inguen	5.0	-	-	+	-	-	-	-
7	50 years	male	pelvic cavity and abdominal wall	Not be measured	-	+	+	-	+	-	+
8	63 years	male	pelvic cavity and inguen	Not be measured	+	-	+	-	-	-	-
9	36 years	female	small intestine	Not be measured	-	-	+	+	-	-	+
10	63 years	female	mesenterium	3.2	-	-	+	-	+	-	+
11	60 years	female	bladder	3.2	-	+	+	-	+	-	-
12	63 years	female	vesicorectal space	4.9	+	-	+	+	-	-	+
13	32 years	male	presacral region and buttocks	Not be measured	+	-	+	-	-	-	-
14	45 years	female	retroperitoneal	18.8	-	+	+	-	+	-	+

Note: + indicates positive result, and – represents negative result.

Table 2 CT Findings in 14 Patients with IMT

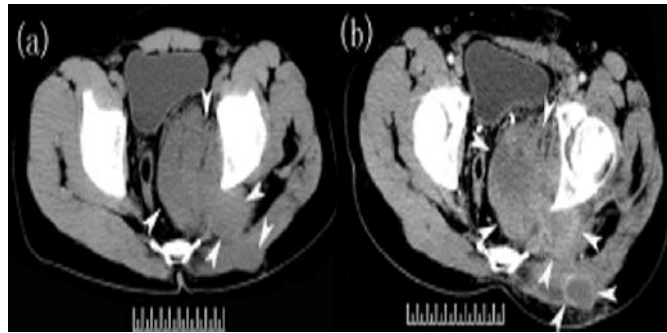
Case	Scan Mode	Shape	Density	Margin	Homogeneity	Calcification	Enhanced Features		Invasion	Complications
							Homogeneity	Degree		
1	plain and enhanced	fusiform	iso-	well-defined	homo-	no	hetero-;small area of cyst	persistent; moderate	no	Intussusception; pelvic effusion
2	plain and enhanced	irregular	iso-	ill-defined	homo-	no	hetero-;small area of more enhancement	persistent; marked	bladder wall and adjacent intestinal canal	no
3	plain and enhanced	oval	hypo-	well-defined	hetero-	no	hetero-;small area of cyst	persistent; slight	no	no
4	plain and enhanced	irregular	iso-	ill-defined	hetero-	no	hetero-;small area of cyst	persistent; marked	no	no
5	plain and enhanced	oval	hypo-	well-defined	hetero- ; cystic-solid	no	hetero-;large area of cyst	persistent; marked	no	adjacent structure shift
6	plain and enhanced	oval	iso-	well-defined	homo-	no	hetero-;small area of cyst	persistent; marked	no	no
7	plain and enhanced	irregular	iso-	ill-defined	homo-	no	hetero-;small area of cyst	persistent; marked	pelvic cavity and adjacent skin	no
8	plain and enhanced	irregular	iso-	ill-defined	hetero- ; cystic-solid	no	hetero-;large area of cyst	persistent; marked	iliopsoas muscle	no
9	plain	/	iso-	/	homo-	no				
10	plain and enhanced	irregular	iso-	ill-defined	hetero- ; cystic-solid	no	hetero- ; ring-shaped enhancement	persistent; marked	no	no
11	plain and enhanced	irregular	hypo-	ill-defined	hetero- ; cystic-solid	no	hetero-;large area of cyst	persistent; marked	no	no
12	plain and enhanced	irregular	iso-	ill-defined	hetero-	no	hetero-;small area of cyst	persistent; marked	bladder wall	bilateral kidney and ureter expansion
13	plain and enhanced	irregular	iso-	ill-defined	hetero-	no	hetero-;small area of cyst	persistent; moderate	the skin of left buttocks	no
14	plain and enhanced	irregular	hypo-	well-defined	homo-	no	hetero-;small area of cyst	persistent; slight	no	no

Fig. 1 IMT of the small intestine in a 36 years female.



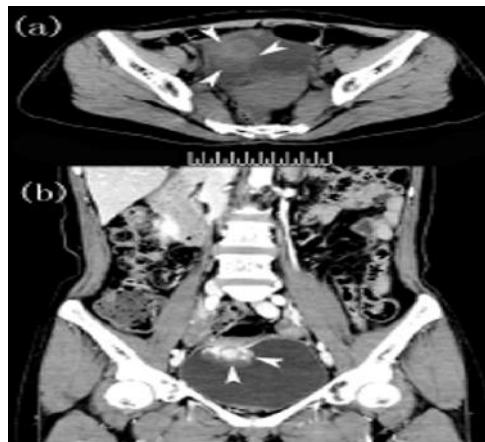
Plain CT images showed focal thickening in the bowel wall (a, b; white arrows).

Fig. 2 A recurrent IMT with multiple lesions in a 32 years male.



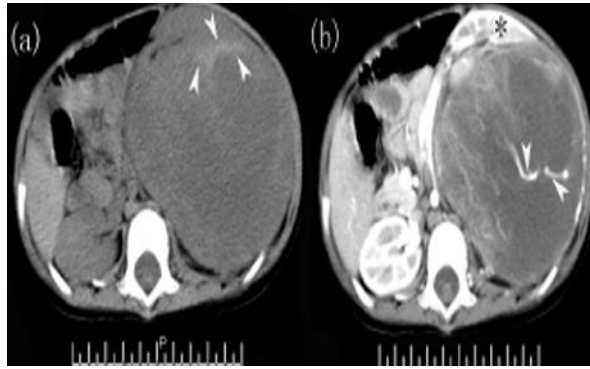
Plain CT image demonstrated multiple lesions in presacral region and buttocks (a; white arrows); enhanced CT image showed moderate enhanced with areas of cyst and thickening of adjacent skin (b; white arrows).

Fig. 3 IMT of the bladder in a 60 years female.



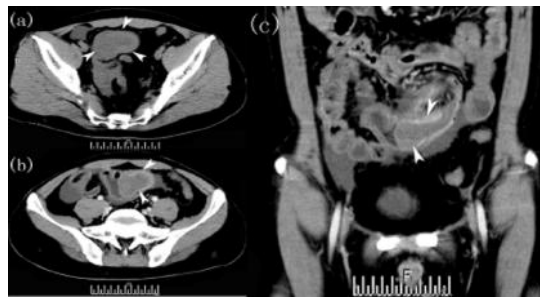
On plain CT image, the lesion exhibited an irregular shape, heterogeneous isodense mass protruding into the lumen (a; white arrows); on enhanced CT images, the lesion was persistent heterogeneous enhanced with multiple areas of cyst (b; white arrows).

Fig. 4 IMT of the left kidney in a 16-month girl.



On plain CT image, the lesion showed an oval hypodense mass with small lamellar hyperdense density (a; white arrows); the lesion was heterogeneous enhanced with a large area of cyst and small nutrient artery after enhancement (b; white arrows; * representing of the left kidney), and adjacent structures were shift.

Fig. 5 IMT of the ileum in a 39 years male.



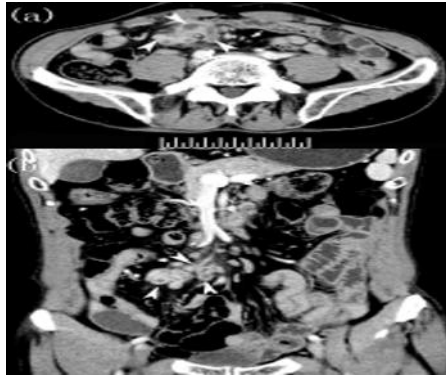
Plain CT image showed an intraluminal hypodense fusiform mass (a, white arrows); enhanced CT images exhibited a moderate enhanced fusiform mass with a complication of intussusception in the small intestine (b, c; white arrows).

Fig. 6 IMT of the pelvic cavity and left inguinal in a 63 years male.



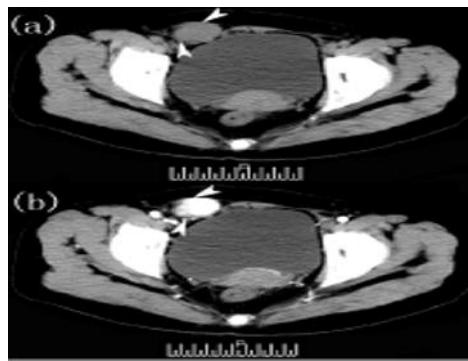
Enhanced CT images demonstrated an irregular marked enhanced mass with multiple large area of cyst (a, b).

Fig. 7 IMT of the mesenterium in a 63 years female.



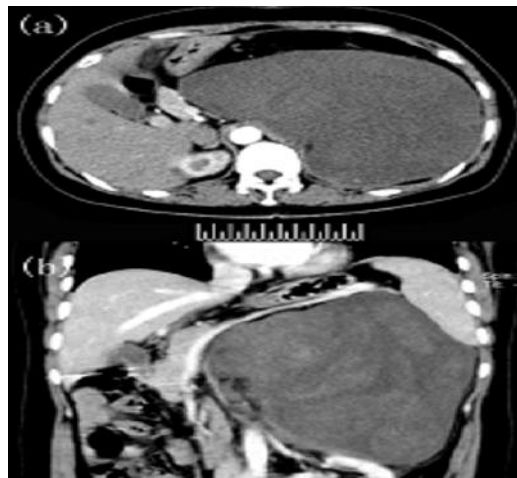
On enhanced CT images, the lesion exhibited multiple ring-shaped enhancements (a, b; white arrows).

Fig. 8 IMT of the right inguen in a 63 years female.



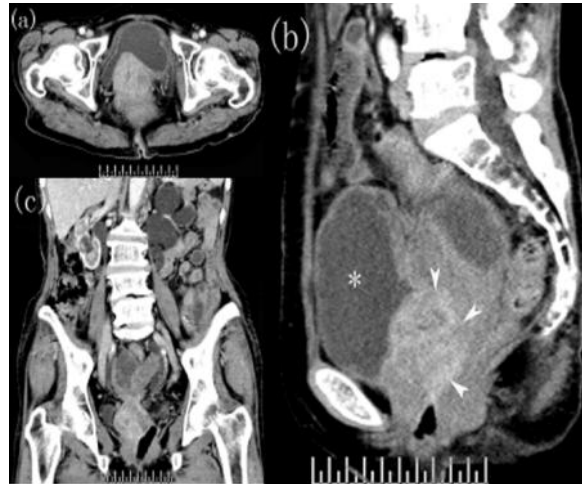
Plain CT image showed a well-defined oval mass (a; white arrows); enhanced CT images demonstrated an enhanced markedly mass, which was misdiagnosed as castleman's disease (b; white arrows).

Fig. 9 IMT of the retroperitoneal region in a 45 years female.



Enhanced CT images demonstrated a huge well-defined, irregular-shaped, slight enhanced mass, and adjacent structures were shift (a, b).

Fig. 10 IMT of the vesicorectal space in a 63 years female.



On enhanced CT images, the lesion exhibited an ill-defined, irregular-shaped, marked enhanced mass with small area of cyst (a), and invasion in adjacent structures were found (b, white arrows; and * representing of the bladder); expansion and hydronephrosis were found in the bilateral kidney and ureter (c).

21, 22). The abdomen and pelvic regions are reported to be the most common locations of extrapulmonary IMT (2, 3, 8), but most of the reported studies are case reports (5-7, 9-15). IMT usually affects young adults and children, with a slight female predominance, but it can occur in any age group. In the present series, there were 8 female and 6 male patients, with an age range of 16 months to 84 years (mean: 45.8 years old). The mean age in our study was slightly higher. This may be caused by the limited number of cases and single location at the intra-abdominopelvic region. IMT predominantly has single lesions, but it may have multiple lesions. In our series, 10 of the 14 patients had a single lesion. Clinically, the presenting symptoms of IMT are typically non-specific and depend on the location of the lesions. In our 14 IMT cases with a lesion arising in the abdominal and pelvic region, 4 patients with lesions located at the gastrointestinal tract showed abdominal pain and distension, each one patient had lesion in the bladder and vesicorectal space that appeared as intermittent gross hematuria, and the other patients showed a mass that mainly lacked the involvement of adjacent organs or superficial locations. Additionally, it has been reported that approximately 20% of the cases are associated with pyrexia, weight loss, an elevated erythrocyte sedimentation rate (ESR) and, occasionally, anemia (2, 3, 7, 18). The size could not be measured in 4 cases of multiple lesions and one case located at the small intestine because of the appearance of bowel wall thickening in our series; the size also depended on the location of the lesions. Generally speaking, the lesions located at the intra-abdominopelvic region are larger than those located

at organs because of the relatively bigger growth space and absence of initial clinical symptoms. Further, the largest lesion in our study, with a maximum diameter of 18.8 cm, was found in the retroperitoneal region. Immunohistochemistry is vital in the assessment of such spindle-cell lesions within IMT lesions. In our study, the immunohistochemical examination revealed that 100%, 35.7% and 35.7% of lesions had positive staining for SMA, vimentin and ALK, respectively. This finding is consistent with other reports in the literatures (4, 18, 23).

The imaging findings of IMT in the abdomen and pelvic region have been reported, but most of them are case reports (5-7, 9-15). In the present study, we demonstrated the imaging findings of 14 cases of IMT in the abdominal and pelvic regions, including the gastrointestinal tract (n=3), retroperitoneal region (n=2), pelvic cavity and abdominal wall (n=2), and one case each in the vesicorectal space, mesentery, kidney, inguinal region, bladder, pelvic cavity and inguinal region, presacral region and buttocks. Cases described at the liver have been commonly presented in the literatures (9, 11), but such cases were excluded from our series because these were usually called inflammatory pseudotumors at our institution, leading to their omission in the selection of patients. Previous studies have described the tumors as large and irregular intraabdominopelvic masses with heterogeneous enhancement and small areas of hemorrhage and necrosis, and the tumors could present as infiltrative or multifocal disease (5-7, 9, 10, 12-15). In our series, the plain CT images showed a soft tissue mass in

all IMT lesions, except for one lesion arising in the small intestine, which had focal thickening in the bowel wall; the majority of mass-like lesions had an ill-defined margin (8/13), irregular shape (9/13), isodense region (9/13), and heterogeneous appearance (8/13). 4 patients had multiple lesions, 7 cases had cystic changes and one patient had hemorrhagic changes. These findings were consistent with the previously cited studies. Calcification is a rare finding in IMT lesions. Few authors have described calcified masses in some pediatric patients with IMT (13, 24), but no calcification was found in our study. This may be due to the relationship with the higher percentage of adult cases in our series (12 of the 14 patients were over 20 years of age). After enhancement, all soft tissue masses were persistently enhanced; they were heterogeneous with various cystic or necrotic regions, including 9 cases that were markedly enhanced and two cases each that were moderately and slightly enhanced, and 3 cases had large-area cystic changes in the marked enhanced masses (with locations at the kidney, bladder, pelvic cavity and inguinal region). This was histologically related to an alternation of the predominantly spindle cell areas with a myxoid-vascular IMT subtype (7), which may be caused by insufficient blood supply in the large soft-tissue masses. There were some rare CT findings in our series. Multiple ring-shaped enhancements were found in one case of mesenteric IMT, which was different from the report by Ko et al (6). One lesion in the inguinal region had a markedly enhanced mass, which our radiologist misdiagnosed as castleman's disease. Similar findings were not previously reported. In our study, a renal IMT showed a huge, markedly enhanced mass with a large area of cystic changes and a small nutrient artery, and the adjacent structures were shifted; it differed from the descriptions of some other authors (12, 25). Two slightly enhanced lesions originated in the retroperitoneal region in our study. Even in the same location, the lesion appearance differed. Additionally, in our study, some lesions that arose in the gastrointestinal tract showed focal thickening in the bowel wall, an irregular mass, and a well-defined fusiform mass with the complication of intussusception. Of our 14 IMT patients, 5 cases showed invasion into adjacent structures, including all four patients with multiple lesions and one single lesion that was located at the vesicorectal space. The rate of invasion in our study was slightly lower than that of the lesions in the head and neck. Yuan et al. (21) described eight cases with bone destruction with infiltration into the nasal fossa, orbit, infratemporal fossa, and other adjacent tissues. No lymph node enlargement was found in our study.

There are few reports on the MRI findings of IMT in the abdominal and pelvic regions (6, 7, 11, 15). The majority of the IMT lesions were isointense on T2-weighted images and had mixed isointense or mild hyperintense lesions, which depended on the percentages of the cell contents and on the contrast-enhanced MR images showing variable enhancement patterns (6, 7, 11, 15). However, these findings are nonspecific, and the final diagnosis is based on the pathology. CT is more commonly used at our hospital, and there is no evidence that MRI is superior to CT in the diagnosis of IMT. No MRI findings were mentioned in our series. Because most abdominal/pelvic IMT cases show large and irregular masses with more aggressive growth patterns that mimic sarcomas, these IMTs need to be differentiated from other abdominal and pelvic malignant tumors, such as malignant fibrous histiocytoma, fibromatosis, or even conventional sarcoma (26, 27). Additionally, if the lesions are located at the organ, the differential diagnosis should be made with the primary malignant tumors of the organ.

IMT has a certain malignant potential, and it may be locally aggressive, recrudescing, and have rare distant metastasis. Currently, surgery aiming at the complete removal of tumor is the main treatment for IMT; however, some cases of IMT may be unresectable due to the deep location and proximity to vital structures. Tumor recurrence usually follows incomplete surgical resection. The prognosis is poor if there is local recurrence because IMT does not respond to chemotherapy and radiotherapy. Hence, follow-up and postoperative monitoring is very important. Unfortunately, we do not have long-term follow-up for this series. Additionally, there was only one case of postoperative recurrence in our study because that was the first time that the patient had visited our institution

after the primary lesion had been removed one year previously at another institution. Confirming a pre-operative diagnosis from radiological features is difficult; however, the CT examination, particularly for contrast-enhanced CT, is helpful in evaluating the location and extent of the tumor and the invasion of adjacent structures and postoperative follow-up.

In summary, the CT features of IMT in the abdominal and pelvic regions are non-specific, and the features differ according to the different locations and the percentages of different histological components in the lesions. IMT can be suspected preoperatively in the case of a huge, ill-defined, irregularly shaped, markedly enhanced mass with

various areas of cystic or necrotic regions in the abdominopelvic region on CT images, mimicking malignancy in the absence of lymph node enlargement, distant metastasis and other malignant signs. However, precise diagnosis should be made based on histopathologic findings. Additionally, the CT examination can be helpful for preoperative assessment and postoperative follow-up.

Conflicts of interest

The authors have no conflicts of interest to declare.

Acknowledgements

The authors thank the patients for their willingness to cooperate with our study, and the pathologic professors who helped us to analyze the histological features of IMT.

References

1. Bahadori M, Liebow AA. 1973. Plasma cell granulomas of the lung. *Cancer*. 31(1):191-208.
2. Coffin CM, Watterson J, Priest JR, et al. 1995. Extrapulmonary inflammatory myofibroblastic tumor (inflammatory pseudotumor). A clinicopathologic and immunohistochemical study of 84 cases. *Am J Surg Pathol*. 19(8):859-872.
3. Coffin CM, Humphrey PA, Dehner LP. 1998. Extrapulmonary inflammatory myofibroblastic tumor: a clinical and pathological survey. *Semin Diagn Pathol*. 15(2):85-101.
4. Fletcher CDM, Unni KK, Mertens F. World Health Organization Classification of tumors. Pathology and genetics of soft tissue and bone. Lyon: IARC Press, 2002: 48-106.
5. Kim KA, Park CM, Lee JH, et al. 2004. Inflammatory myofibroblastic tumor of the stomach with peritoneal dissemination in a young adult: imaging findings. *Abdom Imaging*. 29(1):9-11.
6. Ko SW, Shin SS, Jeong YY. 2005. Mesenteric inflammatory myofibroblastic tumor mimicking a necrotized malignant mass in an adult: case report with MR findings. *Abdom Imaging*. 30(5):616-619.
7. Horger M, Pfannenbergl C, Bitzer M, et al. 2005. Synchronous gastrointestinal and musculoskeletal manifestations of different subtypes of inflammatory myofibroblastic tumor: CT, MRI and pathological features. *Eur Radiol*. 15(8):1713-1716.

8. Kovach SJ, Fischer AC, Katzman PJ, et al. 2006. Inflammatory myofibroblastic tumors. *J Surg Oncol*. 94(5):385-391.
9. Kim SJ, Kim WS, Cheon JE, et al. 2009. Inflammatory myofibroblastic tumors of the abdomen as mimickers of malignancy: imaging features in nine children. *AJR Am J Roentgenol*. 193(5):1419-1424.
10. Rasalkar DD, Chu WC, To KF, et al. 2010. Inflammatory myofibroblastic tumour: an imaging dilemma (2010: 5b). IMFT of the bladder. *Eur Radiol*. 20(8):2057-8.
11. Venkataraman S, Semelka RC, Braga L, et al. 2003. Inflammatory myofibroblastic tumor of the hepatobiliary system: report of MR imaging appearance in four patients. *Radiology*. 227(3):758-763.
12. Boo YJ, Kim J, Kim JH, et al. 2006. Inflammatory myofibroblastic tumor of the kidney in a child: report of a case. *Surg Today*. 36(8):710-713.
13. Rasalkar DD, Chu WC, To KF, et al. 2010. Radiological appearance of inflammatory myofibroblastic tumour. *Pediatr Blood Cancer*. 54(7):1029-1031.
14. Schütte K, Kandulski A, Kuester D, et al. 2010. Inflammatory Myofibroblastic Tumor of the Pancreatic Head: An Unusual Cause of Recurrent Acute Pancreatitis - Case Presentation of a Palliative Approach after Failed Resection and Review of the Literature. *Case Rep Gastroenterol*. 4(3):443-451.
15. Mirshemirani A, Tabari AK, Sadeghian N, et al. 2011. Abdominal inflammatory myofibroblastic tumor: report on four cases and review of literature. *Iran J Pediatr*. 21(4):543-548.
16. Coffin CM, Dehner LP, Meis-Kindblom JM. 1998. Inflammatory myofibroblastic tumor, inflammatory fibrosarcoma, and related lesions: an historical review with differential diagnostic considerations. *Semin Diagn Pathol*. 15(2):102-110.
17. Meis-Kindblom JM, Kjellström C, Kindblom LG. 1998. Inflammatory fibrosarcoma: update, reappraisal, and perspective on its place in the spectrum of inflammatory myofibroblastic tumors. *Semin Diagn Pathol*. 15(2):133-143.
18. Coffin CM, Hornick JL, et al. 2007. Inflammatory myofibroblastic tumor: comparison of clinicopathologic, histologic, and immunohistochemical features including ALK expression in atypical and aggressive cases. *Am J Surg Pathol*. 31(4):509-520.
19. Gleason BC, Hornick JL. 2008. Inflammatory myofibroblastic tumours: where are we now? *J Clin Pathol*. 61(4):428-437.

20. Coffin CM, Patel A, Perkins S, et al. 2001. ALK1 and p80 expression and chromosomal rearrangements involving 2p23 in inflammatory myofibroblastic tumor. *Mod Pathol.* 14(6):569-576.
21. Yuan XP, Li CX, Cao Y, et al. 2012. Inflammatory myofibroblastic tumour of the maxillary sinus: CT and MRI findings. *Clin Radiol.* 67(12):e53-57.
22. Kim JH, Chang KH, Na DG, et al. 2009. Imaging features of meningeal inflammatory myofibroblastic tumor. *AJNR Am J Neuroradiol.* 30(6):1261-1267.
23. Guan Y, Chen G, Zhang W, et al. 2012. Computed tomography appearance of inflammatory myofibroblastic tumor in the mediastinum. *J Comput Assist Tomogr.* 36(6):654-658.
24. Karnak I, Senocak ME, Ciftci AO, et al. 2001. Inflammatory myofibroblastic tumor in children: diagnosis and treatment. *J Pediatr Surg.* 36(6):908-912.
25. Li Z, Wang W, Wang Y, et al. 2013. Inflammatory myofibroblastic tumor of the kidney with viral hepatitis B and trauma: A case report. *Oncol Lett.* 6(6):1741-1743.
26. Karki B, Xu YK, Wu YK, et al. 2012. Primary malignant fibrous histiocytoma of the abdominal cavity: CT findings and pathological correlation. *World J Radiol.* 4(4):151-158.
27. Guglielmi G, Cifaratti A, Scalzo G, et al. 2009. Imaging of superficial and deep fibromatosis. *Radiol Med.* 114(8):1292-1307.